Journal of Molecular Catalysis A: Chemical 165 (2001) 219–230

JOURNAL OF MOLECULAR CATALYSIS A: CHEMICAL

www.elsevier.com/locate/molcata

Hydrogenation of CO over Rh/SiO_2-CeO_2 catalysts: kinetic evidences

C. Mazzocchia [a], P. Gronchi [a], A. Kaddouri [a,*], E. Tempesti [b], L. Zanderighi [c], A. Kiennemann [d]

[a] Chemical Engineering and Industrial Chemistry Department, Politecnico di Milano, P.zza L. Da Vinci, 32 20133 Milano, Italy
[b] Department of Chemistry and Physics for Material Sciences, University of Brescia, Via Valotti 9, 25123 Brescia, Italy
[c] Department of Physical Chemistry and Electrochemistry, University of Milano, Via Venezian 21, 20133 Milano, Italy
[d] LERCSI-ECPM UMR 7515 25, rue Becquerel BP 08 67087 Strasbourg Cedex 2, France

Received 21 June 2000; accepted 11 September 2000

Abstract

The CO hydrogenation over Rh/SiO_2-CeO_2 was investigated kinetically in order to find the rate equation as a function of CO and H_2 partial pressures. Relative to previous findings obtained with Rh/SiO_2 a fairly higher dependence on adsorbed CO is evident. Together with additional evidences found by TPD/TPR and IR spectroscopy, this higher dependence has been tentatively associated to a CO in which both the carbon and the oxygen ends are bonded to Rh and Ce^{3+}, respectively. The influence of the support has been emphasized in order to ascertain the role of CeO_2 (promoter) relative to Rh/SiO_2. In agreement with previous findings we have found that with Rh/SiO_2-CeO_2 catalysts, the promoter inhibits the total activity while favoring the formation of EtOH. © 2001 Elsevier Science B.V. All rights reserved.

Keywords: CO hydrogenation; Rh/SiO_2-CeO_2 catalysts; Promoter; Kinetic

1. Introduction

The formation of oxygenates from carbon monoxide hydrogenation over Group VIII metals has been shown to be quite sensitive to support and promoter composition as well as metal dispersion. Among the different catalytic systems, rhodium based catalysts are the most suitable for the study of the promoter and support interactions that are of great importance in determining the selectivity and activity.

To increase the selectivity in C_2-oxygenated products, the effect of support has been thoroughly investigated, for example with Rh supported on TiO_2 [1], La_2O_3 [2,3], ThO_2 [4] and V_2O_3 [5]. Interesting results for ethanol formation have been observed while conflicting data have been reported for rhodium supported on SiO_2 [6,7] and ZrO_2 [8,9]. As for the promoters and the specific role for syngas conversion to oxygenated products, various contributions [10–13] have been made.

Recent workers have claimed that the promoters and/or the supports influence the adsorption of carbon monoxide. An adsorption mode of carbon monoxide was observed on promoted catalysts [10,14–18] in which both the carbon and the oxygen ends of the CO moiety are bonded to the catalytic surface. An extensive review has been published on the subject [19].

* Corresponding author. Tel.: +39-2-23993247; fax: +39-2-70638173.
E-mail address: akim.kaddouri@polimi.it (A. Kaddouri).

1381-1169/01/$ – see front matter
PII: S1381-1169(00)00425-8

More specifically the studies of the particle size [20,21] have evidenced partial coverage of the metal particles by patches of promoters or support.

Another unsolved problem is the influence of the promoters on the carbon–carbon bond formation. An acyl intermediate [22–24] has often been proposed to be the key to the C_2-oxygenate formation. Additional evidences are now discussed in order to explain the reactivity and selectivity tests performed on $Rh/CeO_2/SiO_2$ catalysts.

Another aim of the present study is to find additional kinetic evidences on the role of cerium oxide in ethanol promotion.

2. Experimental

2.1. Catalyst preparation

The catalyst was prepared by incipient wetness method using SiO_2 (Roth 0201; 100 mesh) and a solution (0.6 g in 5 ml of distilled water) of $RhCl_3 \cdot nH_2O$ (Johnson Mattey; 42.5% Rh) and $Ce(NO_3)_3 \cdot 6H_2O$ (Fluka) which correspond to the percentage of CeO_2 desired. The solution (mixture of Rh and Ce salts) was brought into contact with silica, under vacuum. After leaving the catalyst in air for 30 min, it was dried at 333 K for 30 min, under argon, and then at 433 K overnight. Finally, the catalyst was calcined at 823 K during 6 h. Rhodium crystallite size (by H_2/O_2 adsorption): $Rh/SiO_2\text{-}CeO_2$ = 43–46 Å.

2.2. Apparatus and procedures

Catalytic runs were performed in a stainless steel (AISI 316) tubular reactor (length 45 cm, i.d. 0.8 cm) heated in a ventilated oven. A thermocouple was placed in the middle of the catalytic bed which was prepared by blending (1:30) the catalyst with carburundum (>200 mesh) to obtain better control of the temperature; carburundum was also added to fill the reactor. A temperature range of 473–530 K under a total pressure ($P_{H_2} + P_{CO}$) of 1 atm was investigated using different sets of experiments. The effects of partial pressure were analyzed for $H_2/CO = 1$–5 by dilution with He. Low conversions were obtained by varying the space velocity (SV) of the feed. Runs were performed using CO, H_2 and He and varying the gas ratios by flow mass controllers (Brooks). 99.99% pure H_2 was used to activate the catalyst ($T = 648$ K, $F = 4\,l\,h^{-1}\,g_{cat}{}^{-1}$ during 16 h).

2.3. Analyses

One milliliter of reacted gas mixture was sampled periodically in a heated (383 K) eight-port on-line valve and analyzed simultaneously by two chromatographs equipped with hot wire detectors (H_2 carrier gas $1.5\,l\,h^{-1}$) (A) analysis of volatile products — Porapack QS column (length 4 m, i.d. 2 mm), isothermal at 303 K; (B) analysis of C_1–C_6 fractions — Porapack R column (length 6 m, i.d. 2 mm), isothermal at 413 K.

Data were obtained on the basis of identified products having a retention time less than 45 min from type B analysis. Carbon efficiency was calculated by the formula $n_i / \sum n_i C_i$ where n_i is the carbon atom number of the C_i compound. The analytical results adequately satisfied material balance.

2.4. Temperature-programmed desorption (TPD) and reduction (TPR)

For TPD runs CeO_2, Rh/CeO_2, Rh/SiO_2 and $Rh/CeO_2\text{-}SiO_2$ samples were reduced with H_2 for 3 h at 573 and 723 K and cooled under He flow to ambient temperature. CO (0.1 MPa) was fed up to saturation at the same temperature and then desorbed at increasing temperature ($6\,K\,min^{-1}$) in flowing He ($2\,l\,h^{-1}\,g_{cat}{}^{-1}$). The TPD/TPR runs on Rh/CeO_2 have been investigated by preliminary adsorbing CO at 403 K up to saturation followed by cooling at room temperature. The sample was heated up to 423 K under He flow (TPD) and again cooled to room temperature. TPR runs were carried out by heating under H_2 flow after (TPD). The desorbed products were analyzed simultaneously by two chromatographs, using HWD detector for CO and CO_2 and a FID detector for CH_4. Successively a catharometer was used to have the total gaseous product concentration. Accordingly, no direct quantitative correlation can be made between CO, CO_2 and CH_4.

3. Results

3.1. TPD experiments

According to literature [25,26], CO, CO_2 and CH_4 have been observed during TPD experiments on CeO_2, Rh/CeO_2, Rh/SiO_2 and Rh/SiO_2-CeO_2 catalysts.

On pure CeO_2 it results that (Fig. 1):

- CO_2 desorption begins at ca. 380 K and will continue till high temperature.
- CO desorbs in the temperature range 500–750 K.
- CH_4 formation occurs at high temperature (630 K).

The TPD desorption of CO_2 occurs at lower temperature, and in two steps, by adding 5% of Rh on CeO_2 (see Fig. 2a II relative to Fig. 1). The first desorption peak is observed at ca. 370 K in the region of CO desorption; the second desorption peak at high temperature, coincides with the maximum peak of CH_4. Only the high temperature CO_2 desorption peak (at ca. 610 K) is observed with 5% Rh/SiO_2 catalysts (see Fig. 2a I), exactly at the same temperature of the methane peak. CO shows a low temperature desorption peak at ca. 370 K, and a high temperature desorption peak at 473 K, assigned to strongly adsorbed CO. By adding CeO_2 to Rh/SiO_2 catalysts (see Fig. 2a III, IV, V and VI) the low temperature CO_2 peak is observed in the temperature range of CO peak, and the high temperature CO_2 peak appears at the same temperature of methane peak (ca. 610 K with 5% Rh/SiO_2). It has to be pointed out that, by increasing the amount of CeO_2 from 0 to 5% (see Fig. 2a, b), the maximum of high temperature peak, both for CO_2 and CH_4, is shifted to lower temperatures.

From the TPD data it is thus possible to conclude that:

- the low temperature CO_2 formation implies the dissociation of chemisorbed CO;
- the high temperature CO_2 formation is paralleled by the CH_4 formation and this implies the CO reaction with surface hydroxyl groups to yield methane and water;
- this latter reacts further with CO yielding CO_2 and hydrogen.

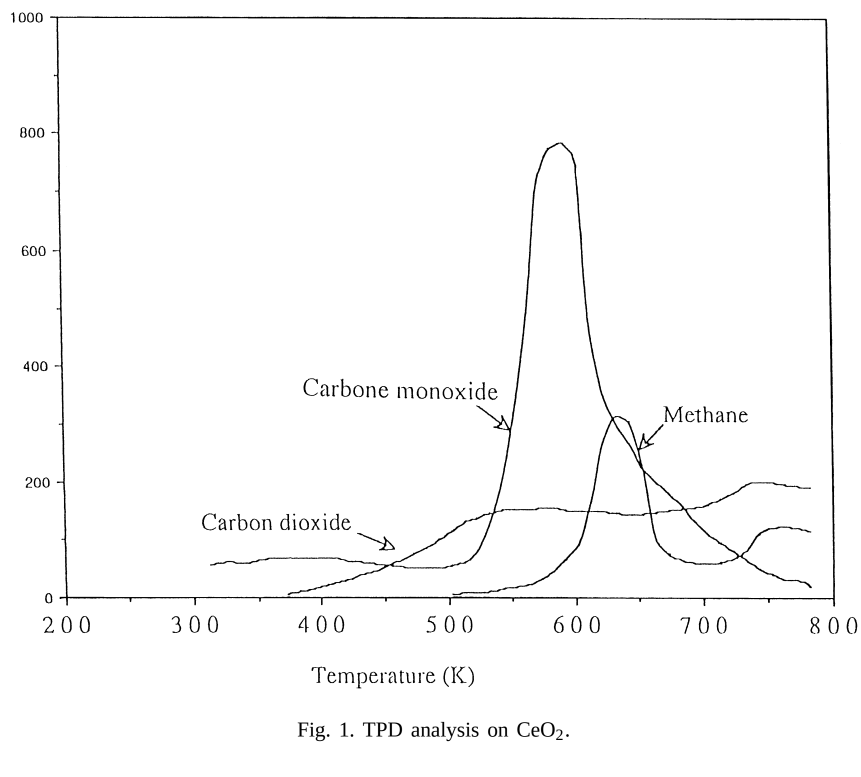

Fig. 1. TPD analysis on CeO_2.

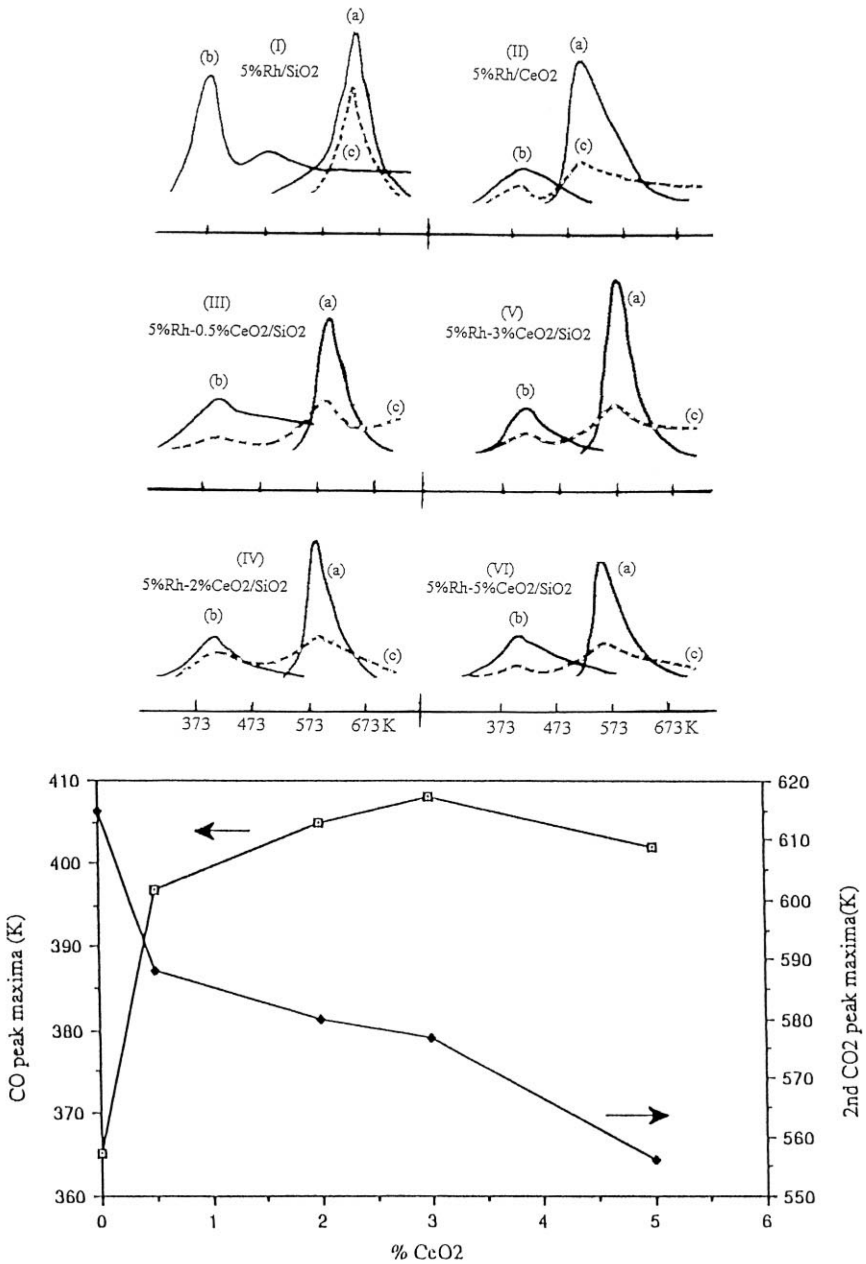

Fig. 2. (a) TPD analysis on Rh/SiO_2, Rh/CeO_2 and $Rh/CeO_2/SiO_2$ catalysts: (a) CH_4; (b) CO; and (c) CO_2. (b) Shift of CO and second CO_2 TPD peak maximum with CeO_2 (percent).

3.2. TPD/TPR experiments

Consecutive TPD/TPR experiments have been performed on Rh/CeO_2, Rh/SiO_2-CeO_2, Rh/SiO_2 catalysts in the temperature range 298–773 K. Fig. 3 reports the TPD/TPR data on Rh/CeO_2. TPD performed in the temperature range 298–400 K shows only a small peak probably due to carbon monoxide and

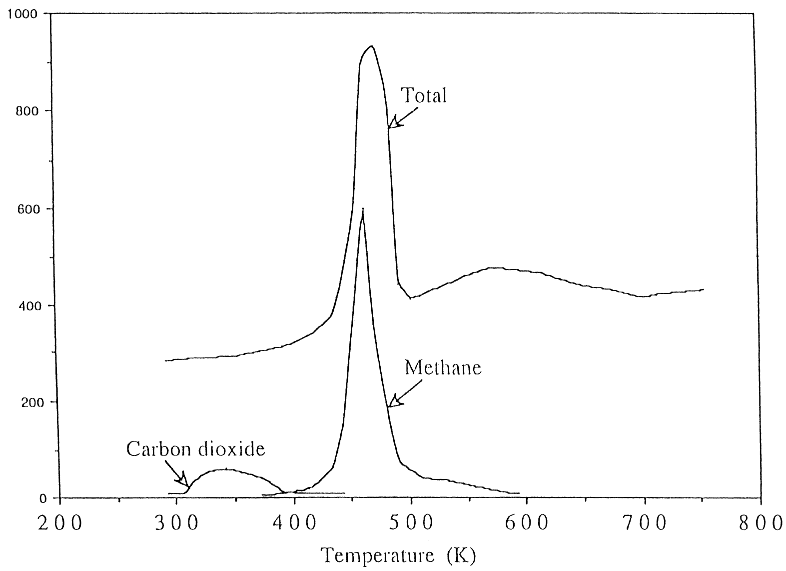

Fig. 3. TPD/TPR analysis on Rh/CeO_2 catalyst.

carbon dioxide desorption. The total response of the following TPR experiment shows two desorption peaks: a very large peak at 480 K followed by a wide peak with a maximum at 570 K. No carbon dioxide is evidenced in these runs. From the difference of the total desorption response observed at 570 K and that of methane at 480 K it may be concluded that, owing to the parallel formation of water, this latter partially desorbs with methane while the more strongly bound water desorbs at higher temperatures.

Fig. 4a shows the total responses of TPD, TPR, and TPR after TPD at $T > 423$ K on Rh/SiO_2-CeO_2, and (Fig. 4b) the methane response in the same runs. The total initial TPD response shows two peaks: one at low temperature (388 K) and the second one at 548 K. Methane is observed only at high temperature. The TPR experiments carried out consecutively shows, a total response (Fig. 4a), a wide flat peak with a maximum at ca. 448 K. The trend of this response is similar to that of methane (Fig. 4b) and no particular suggestions can thus be drawn. TPR experiments performed after treatment in He at $T = 423$ K shows a total response which almost coincides with the methane response while the different evidences are probably due to water since carbon dioxide has not been detected.

CH_4 formation during runs performed after TPD at high temperature (773 K) can be explained only on the basis of hydrogen reaction with surface carbon formed in the previous TPD experiments. This suggests that, during the thermal treatment, the chemisorbed CO would partially dissociate with formation of surface carbon and oxygen. This last species in inert atmosphere reacts with CO to CO_2.

The TPR/TPD total desorption response on Rh/SiO_2 is reported in Fig. 5a. Both experiments show two peaks: the first one occurs at 373 K for both while the high temperature peak occurs at 508 and at 603 K, respectively for the TPR and TPD experiments. The responses of CO, CO_2 and CH_4 are shown in Fig. 5b. CO has a continuous desorption only in TPD experiments while it is totally absent in the TPR experiments. CO_2 is present at low temperature (298–473 K) in TPR runs and at high temperatures (523–773 K) in the TPD experiments. As for CH_4 in the TPD runs, it is present only in traces at high temperature (around 573 K). In TPR experiments, CH_4 is present at 423 K, with a maximum at 498 K ca.; its formation continues up to 773 K. This suggests that methane is formed not only by CO reaction but also by surface C reaction formed in the previous desorption in He stream.

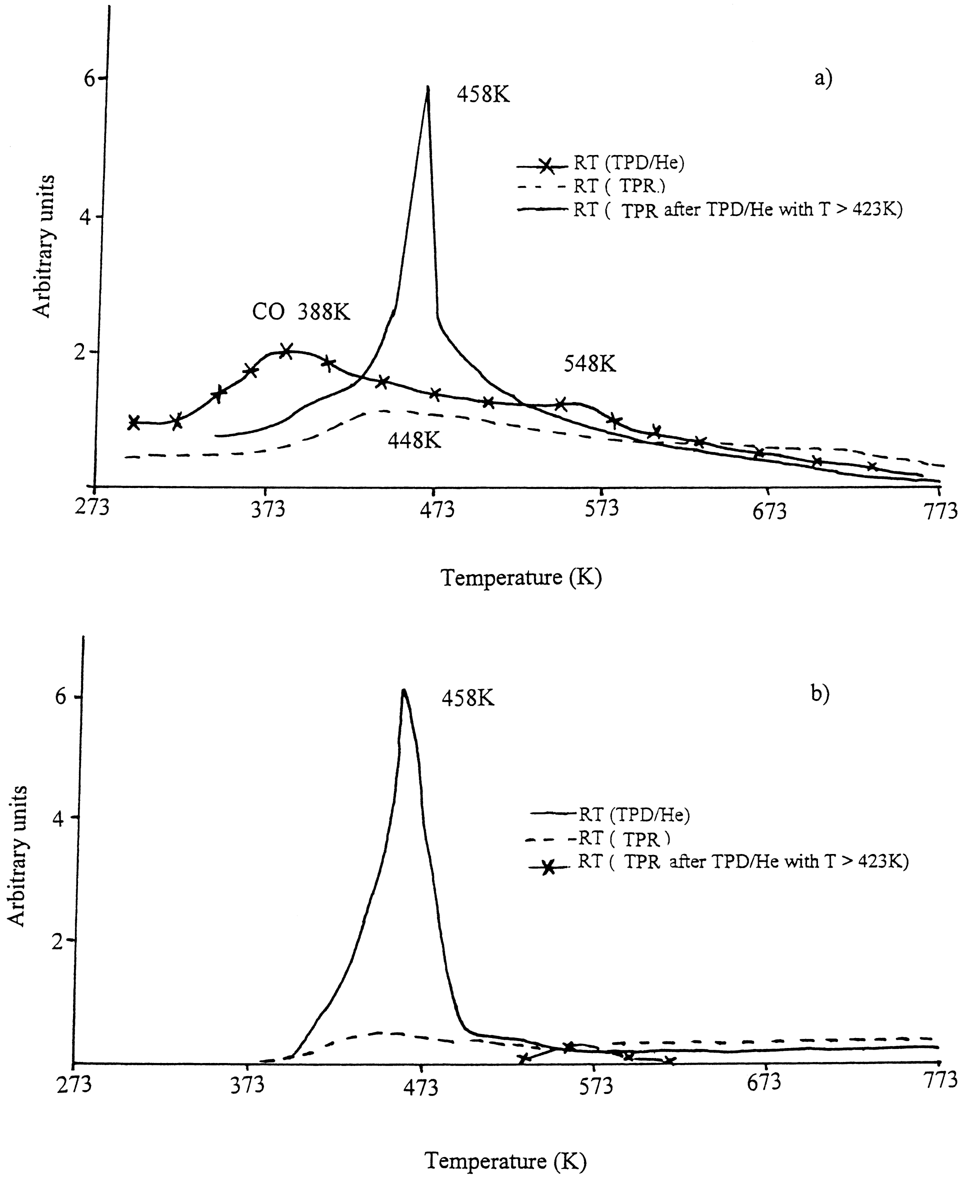

Fig. 4. TPD/TPR analysis on Rh/CeO_2/SiO_2 catalyst: (a) total desorption; (b) methane.

3.3. Kinetic data and parameters

The experimental results of CO hydrogenation under different experimental conditions are reported in Table 1. The kinetic parameters obtained by regression analysis with the following pseudo-homogeneous equation

$$r = k_0 \exp^{-E/RT} P_{H_2}^m P_{CO}^n$$

are reported in Table 2. It results that for the Rh/SiO_2-CeO_2 catalyst the hydrogen partial pressure positively affects both the CO disappearance and the product formation (CH_4–C_2H_5OH), while the CO partial pressure has no influence on the rate of EtOH

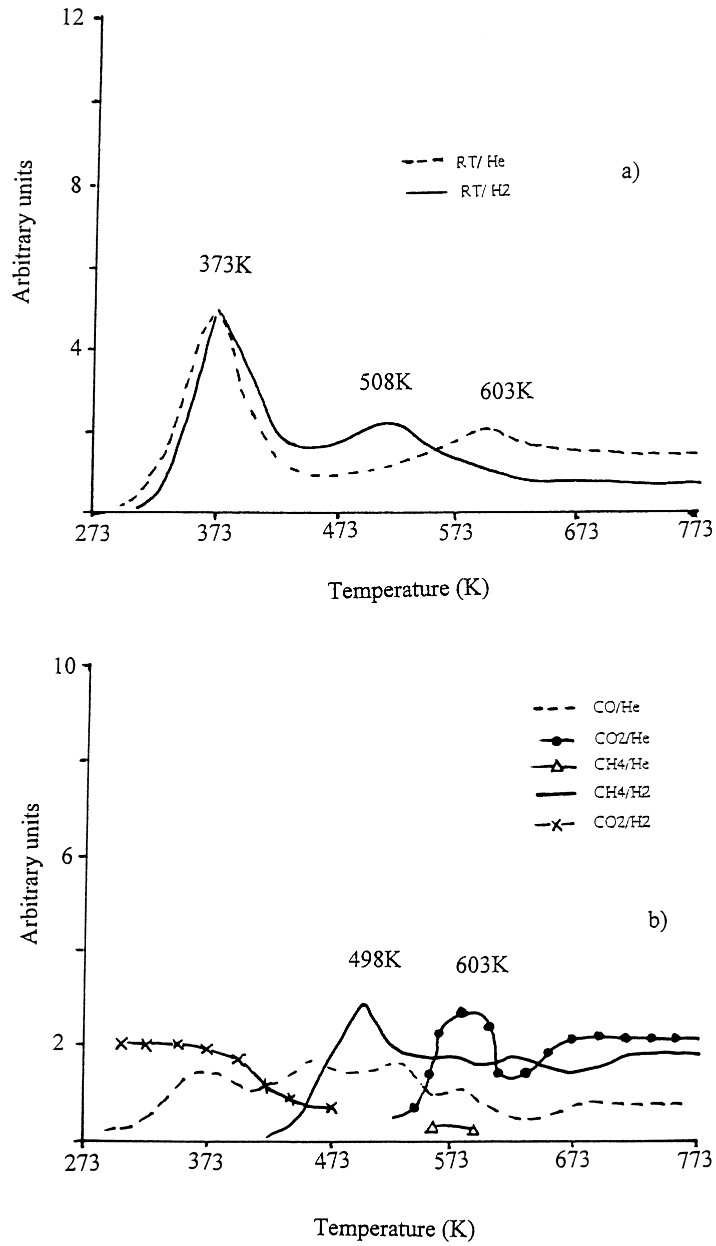

Fig. 5. TPD/TPR analysis on Rh/SiO_2 catalyst: (a) total desorption; (b) methane analysis.

formation but it decreases both the CO disappearance and the CH_4 formation rate. This is further confirmed by considering for the sake of comparison typical kinetic parameters obtained by other authors [35] with Rh/SiO_2 catalysts. Indeed, it may be seen that the absence of the promoter (CeO_2) favors the formation of CH_4.

Table 3 reports the results obtained with 5% Rh/SiO_2 or 5% Rh/SiO_2-CeO_2 (5%) under comparable experimental conditions. CeO_2 reduces drasti-

Table 1
CO conversion and carbon efficiency on Rh/SiO_2-CeO_2 for various H_2/CO ratios and space velocity[a]

T (°C)	H_2/CO	$P_{H_2} + P_{CO}$ (mm Hg)	F/W (ml/g cat.)	Conv. (%)	Carbon efficiency					
					CH_4	HC_{tot}	EtOH	MeOH	AcH	CO_2
200	1	253	3	2.2	32.0	46.9	35.6	6.1	1.1	10.3
220	1	253	6	3.9	37.9	60.2	27.5	2.7	1.9	7.7
235	1	253	6	9.9	46.9	74.2	17.8	2.2	1.3	4.5
200	3	506	3	3.1	40.5	54.6	30.7	7.1	nd	7.6
220	3	506	6	6.2	45.2	60.0	28.1	5.2	2.4	4.3
235	3	506	10	8.3	54.8	70.0	19.4	3.7	3.2	3.7
200	1	760	6	0.8	31.2	45.6	27.5	14.3	nd	12.6
220	1	760	6	1.5	33.5	46.8	36.1	5.9	3.3	7.9
235	1	760	10	1.8	40.7	56.5	30.2	4.3	3.5	5.5
200	3	760	3	2.4	37.2	50.6	36.3	7.9	nd	5.2
220	3	760	5	6.9	56.6	64.5	25.7	4.5	2.4	2.9
235	3	760	10	8.1	60.0	72.5	18.7	3.1	3.4	2.3
200	5	760	6	3.5	46.5	55.9	32.3	7.9	nd	3.9
220	5	760	11	7.6	56.7	63.2	25.2	6.8	2.9	1.9
235	5	760	16	13.2	61.6	75.0	16.7	4.5	2.2	1.6

[a] $(n_i C_i \times 100/\sum n_i C_i)$ where n_i is the carbon atom number of the C_i compound.

Table 2
Kinetic parameters $r = A \exp^{-E/RT} P_{H_2}^m P_{CO}^n$

Catalyst	Species	A[a]	E[a]	m	n
5% Rh/CeO_2 (5%)/SiO_2	CO	9.30×10^8	19.4	0.42	−0.30
	CH_4	0.01×10^{12}	22.1	0.62	−0.77
	EtOH	2.03×10^4	11.8	0.46	0.05
1% Rh/SiO_2 [35]	CH_4	4.1×10^{6}[b]	22.6	0.57	−0.20
1% Rh/ZrO_2 [23,33,34]	CO	360×10^8	25.4	0.35	−0.94
	CH_4	180×10^{12}	34.3	0.65	−1.44
	EtOH	6.1×10^4	15.8	0.43	−0.53

[a] A: mol h^{-1} gRh^{-1} atm$^{-(m+n)}$; E: kcal mole^{-1}.
[b] Expressed in (s^{-1} atm$^{-(m+n)}$).

Table 3
Effect of promoter on the carbon efficiency[a]

Catalyst	Conv. (%)	Carbon[b] (%) efficiency						Reference
		CH_4	HC_{tot}	EtOH	MeOH	AcOH	CO_2	
Rh (5%)/SiO_2	11.2	64.1	91.8	0.7	0.4	7.1	n.d.	This study
Rh (5%)/CeO_2 (5%)/SiO_2	3.1	40.5	58.6	30.7	7.1	n.d.	7.6	This study
Rh (5%)/ZrO_2 (3%)/SiO_2[c]	4.5		46.8	50.3		2.8		[25]

[a] Reaction temperature = 473 K; H_2/CO = 3; P_{tot} reagents = 498 mm Hg; gas flow = 0.5 l/h g_{cat}.
[b] Carbon efficiency = $(n_i C_i \times 100/\mathrm{S}n_i C_i)$ where n_i is the carbon number of the C_i compound).
[c] H_2/CO = 2; gas flow = 2 l h^{-1} $g_{cat}{}^{-1}$.

cally the activity while the selectivity to ethanol and methanol is sensibly increases (almost 10 folds in terms of overall C_1–C_2 alcohol yield evaluated as the product of carbon efficiency and the conversion). Also the CO_2 formation increase while acetaldehyde is no longer observed.

4. Discussion

The two-step CO_2 desorption observed in TPD runs with Rh/CeO_2/SiO_2 (Fig. 2a III, IV, V and VI) have been observed by other authors on differently Rh supported samples. For instance, in the case of Rh/SiO_2-La_2O_x [27] a broad low temperature peak is observed below 500 K followed by a larger peak above 500 K. A similar behavior has also been reported for Rh/ZrO_2 [23]. In order to understand how the promoter (CeO_2) influences the behavior of carbon monoxide from ambient to high temperatures it is necessary to consider some previous findings. Indeed, from IR data of carbon monoxide hydrogenation over Rh/SiO_2, Rh/CeO_2/SiO_2 and Rh/CeO_2 catalysts it has been shown [15] that the following CO adsorbed species are present at ambient temperature: linear monocarbonyl Rh(CO) (I), gem-dicarbonyl $Rh(CO)_2$ (II), CO-bridged Rh–CO–Rh (III) and C– and O– bonded Rh–CO–M (IV) species. The formation of IV has been explained assuming a CeO_2 reduction near the patches borderline on the metal particle (a redox mechanism $Ce^{4+} \rightarrow Ce^{3+}$ promoted by Rh) with the formation of a dual site chemisorption system Rh–C=O–Ce [28]. On increasing the temperature only the adsorption of species I and IV are evident and significantly the adsorption of the latter species increases. Thus, the two peaks which characterize the CO_2 desorption may be attributed to a CeO_2 promoted: (1) CO dissociation at $T < 500$ K which lead to CO_2 according to the Boudouard [29] reaction ($2CO \rightarrow C + CO_2$ or (2) CO interaction with surface OH at higher temperatures. In the latter case, the surface carbon formed at lower temperatures is hydrogenated further to methane by reacting either with OH groups or with produced hydrogen. These mechanisms are supported by the observation that the maximum CO_2 peak of the second step fairly parallels the maximum peak of CH_4.

As for the observed increase of the maximum CO desorption temperature on increasing the CeO_2 wt.% on SiO_2 surface (Fig. 2b) it may be due to an increased interaction with Rh–CO bonds while the temperature decrease of the second CO_2 desorption peak suggest an increased CO reactivity with surface hydroxyls.

Chemisorbed CO may dissociate directly

$$CO_\sigma + \sigma' \rightarrow C\sigma + O\sigma' \tag{1}$$

to O_σ and C_σ which is thoroughly hydrogenated to CH_x or alternatively with (chemisorbed) hydrogen participation as follows:

$$xH_\sigma + (CO)_\sigma \rightarrow (CH_{x-1})_\sigma + OH_\sigma \tag{2}$$

4.1. Direct CO dissociation

In the first approach, σ' may differ from CO adsorption sites being an Rh site or near to the borderline of the patches (e.g. Ce^{3+}). Under equilibrium conditions it may be assumed that

$$\Theta_C \times \Theta_O = (b_{CO}P_{CO})\Theta_V^2 \tag{3}$$

where Θ_V is the fraction of free sites.

1. If $\sigma' = \sigma$ and assuming that $\Theta_C = \Theta_O$, the carbon coverage may be expressed as follows:

$$\Theta_C = \frac{\sqrt{b_C b_{CO} P_{CO}}}{(1 + b_{CO}P_{CO} + \sqrt{b_H P_H} + 2\sqrt{b_C b_{CO} P_{CO}})} \tag{4}$$

Where b_C is the equilibrium dissociation constant of adsorbed CO. Accordingly the surface reaction between carbon and dissociated hydrogen is

$$r_{CO} = k_{CO}\frac{\sqrt{b_C b_{CO} P_{CO}}\sqrt{b_H P_H}}{(1 + b_{CO}P_{CO} + 2\sqrt{b_C b_{CO} P_{CO}} + \sqrt{b_H P_H})^2} \tag{5}$$

If under the reaction conditions CO is strongly adsorbed and its surface concentration approaches saturation, then the main surface moiety is dissociated CO and

$$2\sqrt{b_C b_{CO} P_{CO}} \gg 1 + b_{CO}P_{CO} + \sqrt{b_H P_H} \tag{6}$$

while the rate equation becomes:

$$r_{CO} = k_{CO}\frac{P_H^{0.5}}{P_{CO}^{0.5}} \tag{7}$$

in fair agreement with the experimental results. According to this model, the rate-determining step is the surface reaction between C_σ and H_σ. CO is adsorbed both in undissociated and dissociated form, the latter being the predominant. Also the surface concentration of hydrogen is low.

2. If σ is a Rh adsorption site and σ' a reduced cerium site near the borderline of the Rh particle, the following assumption has to be introduced:

$$\Theta_C = \Theta'_O \tag{8}$$

In other words, the fraction of Rh particles covered by C is equated to the fraction of surface cerium oxide covered by O. Assuming that the rate-limiting step is the surface reaction of the adsorbed carbon it results:

$$r = k_S \frac{(b'_C b_{CO} b_H P_H P_{CO})^{1/2} \times (1 + (b_H P_H)^{1/2} + (b_{CO} P_{CO}))^{1/2}}{[(1 + (b_H P_H)^{1/2} + b_{CO} P_{CO})^{1/2} + (b'_C b_{CO} P_{CO})^{1/2}]^2} \tag{9}$$

where b'_C is the equilibrium dissociation constant of adsorbed CO.

If $b_{CO} P_{CO} \gg b_H P_H$ then $r = f(P_H^{1/2})$ while if $b_H P_H \gg b_{CO} P_{CO}$ it results that $r = f(P_{CO}^{1/2})$. Both limiting cases are not compatible with the experimental results.

4.2. Hydrogen assisted CO dissociation

Assuming that the rate limiting CO dissociation is promoted by hydrogen, the following rate equation is obtained:

$$r_{CO} = k' \frac{b_{CO} P_{CO} (b_H P_H)^{x/2}}{[1 + b_{CO} P_{CO} + (b_H P_H)^{1/2}]^{x+1}} \tag{10}$$

Assuming that

$$(b_{CO} P_{CO}) \gg (b_H P_H)^{x/2+1} \tag{11}$$

it results

$$r_{CO} = \frac{k'' P_{H_2}^{x/2}}{P_{CO}^{x}} \tag{12}$$

while if $b_{CO} P_{CO}$ may be neglected and

$$(b_H P_H)^{1/2} \gg (1 + b_{CO} P_{CO}) \tag{13}$$

then Eq. (10) becomes:

$$r_{CO} = k \left(\frac{b_{CO} P_{CO}}{(b_H P_H)^{x/2}} \right) \tag{14}$$

Eq. (14) is clearly incompatible with the experimental results while Eq. (12) if $x = 1$, fairly reminds (see Table 2) the results obtained with Rh/ZrO_2 catalysts:

$$r_{CO} = k' X_{H_2}^{0.35} X_{CO}^{-0.94} P_{tot}^{-0.59}. \tag{15}$$

rather than those obtained with $Rh/CeO_2/SiO_2$ catalysts

$$r_{CO} = k X_{H_2}^{0.42} X_{CO}^{-0.30} P_{tot}^{0.11} \tag{16}$$

While in the former case CO has a stronger inhibiting effect on the overall reaction rate, the role of adsorbed hydrogen is apparently similar in both cases. Nevertheless, it should be observed (see Table 2) that the CO, CH_4 and EtOH frequency factors on $Rh/CeO_2/SiO_2$ catalysts are two, five and one order of magnitude, respectively lower than on Rh/ZrO_2 catalysts together with the corresponding activation energies which follow the same trend.

For the Rh/ZrO_2 catalysts the kinetic evidences reported above seem to remind a suggestion proposed by Bell [30] on the basis of isotopic studies which assume hydrogen participation

$$(COH_n)_\sigma \rightarrow (CH_x)_\sigma + OH_\sigma \tag{17}$$

for the CO dissociation catalyzed by transition metals, with $x = n - 1$ and n varying according to the metal.

New spectroscopic evidences have been obtained which seem to support the hydrogen assisted CO dissociation reported above. Indeed, a direct interaction of H_2 (g) with chemisorbed CO on Rh/SiO_2 has been reported [15], which involves H_2 in a reversible ligand process such as

$$Rh^I(CO)_2 \xrightarrow{H_2} Rh^I(H)(CO) \tag{18}$$

This induces a structural rearrangement where atomically dispersed Rh^I sites are reduced and clustered to form larger metallic crystallites.

With $Rh/CeO_2/SiO_2$ catalysts, it has already been anticipated from IR data that the main effect of ceria is the formation of CO species adsorbed in such a way that the carbon end of the molecule is attached to Rh and the oxygen to a Ce cation:

Rh/C=O\X (X = CeO_2)

It is possible to discuss the results obtained in terms of reactivity in relation to the formation of these C– and O– bonded species. Indeed referring to the data obtained in this study reported in Table 3 it may be seen that on passing from 0 to 5% CeO_2 a sensible increase of oxygenated products is observed together with a drastic decrease of CO conversion to methane and hydrocarbons. A similar behavior is found in literature for 5% Rh/3% ZrO_2/SiO_2 [25]. On the other hand, always in agreement with the same findings [25], our TPD results on ceria containing catalyst point to an easier CO dissociation as compared to unpromoted catalyst. This seems at odds with the decreased conversion to methane and hydrocarbons and can be reconciled only if the carbon formed by CO dissociation is assumed to be less reactive on ceria-containing catalysts than on Rh/SiO_2 [15,31]. The formation of a less reactive carbon has also been reported by Rieck and Bell [32] for La_2O_3-promoted Pd/SiO_2. The C and O coordination and the decreased hydrogenation rate of carbon or carbonated species could enhance the selectivity to oxygenated compounds. If it may be safely assumed [28] that the formation of an oxyphil Ce^{3+} at Rh–CeO_2 interface leads to C– and O– bonded species next to the borderline, then the Rh–CO bond should be more available for H_σ or $(CH_x)_\sigma$ insertion reactions leading to formyl or acyl species.

Finally, referring again to the data reported in Table 3 for 5% Rh/SiO_2-CeO_2 catalysts the equations for ethanol and methane formation can be used to define the selectivity S as follows:

$$S = \frac{r_{EtOH}}{r_{CH_4}} = k_S P_{H_2}^{-0.16} P_{CO}^{0.82} = k_S X_{H_2}^{-0.16} X_{CO}^{0.82} P_{tot}^{0.66} \tag{19}$$

while for 1% Rh/ZrO_2 catalysts the following equation is found:

$$S = k'_S P_{H_2}^{-0.22} P_{CO}^{0.91} = k'_S X_{H_2}^{-0.22} X_{CO}^{0.91} P_{tot}^{0.69} \tag{20}$$

In both cases, an increase of the H_2 partial pressure negatively affect the EtOH selectivity while on increasing the CO partial pressure the reverse is true. Both catalytic systems have a similar dependence on total pressure.

In agreement with earlier findings [22] ethanol formation occurs through an acyl intermediate

$$(CH_3)_\sigma + CO_\sigma \rightarrow CH_3CO_\sigma \tag{21}$$

As an alternative to Eq. (21) methane formation may be derived by interacting adsorbed hydrogen and the CH_3 moiety on the surface:

$$(CH_3)_\sigma + H_\sigma \rightarrow CH_{4\sigma} \tag{22}$$

The selectivity may thus be redefined as:

$$S = \frac{r_{EtOH}}{r_{CH_4}} = \frac{k_{EtOH}\Theta_{CH_3}\Theta_{CO}}{k_{CH_4}\Theta_H\Theta_{CH_3}} = \frac{k'\Theta_{CO}}{\Theta_H} \tag{23}$$

Assuming that surface concentration of chemisorbed CO, Θ_{CO}, and that of dissociatively chemisorbed hydrogen Θ_H, are given respectively by:

$$\Theta_{CO} = b_{CO} P_{CO} \Theta_V; \qquad \Theta_H = b_H \cdot P_{H_2}^{1/2} \Theta_V \tag{24}$$

Eq. (23) becomes

$$S \propto \frac{P_{CO}}{P_{H_2}^{1/2}} = X_{CO} X_{H_2}^{-0.5} P_{tot}^{0.5} \tag{25}$$

which fairly reminds the experimental results.

5. Conclusions

The previous discussion allows to draw the following considerations:

1. The addition of CeO_2 on SiO_2 shifts CO hydrogenation to oxygenates, mainly ethanol.
2. The $Rh/CeO_2/SiO_2$ system, at least in the range of the studied experimental conditions, has carbon efficiency values quite similar to those of the Rh/ZrO_2 catalysts.
3. A comparison between $Rh/CeO_2/SiO_2$ and Rh/ZrO_2 indicates that the former system has a lower number of surface active sites and a lower activation energy moreover the inhibiting effect of CO is lower on the $Rh/CeO_2/SiO_2$ catalysts.
4. The mechanism of CO activation and reaction on $Rh/CeO_2/SiO_2$ is probably different from that on Rh/ZrO_2. While on the former the CO adsorption occurs either as CO carbonyl or bridging-carbonyl-bonded, and this last moiety play a key role in the CO reaction path, on Rh/ZrO_2 it seems highly probable that the CO adsorption occurs as CO carbonyl or bridged CO and the reaction path is characterized by CO dissociation assisted by hydrogen.

Finally, we would like to remark that, even if the interaction of CO with the surface sites of the various catalysts (CO dissociation, CO dissociation-assisted or promoted by hydrogen, bridged CO etc.) and its activation and reaction pathway are different, the main reaction steps to oxygenates are similar on all catalysts since all of them implies an acyl intermediate through the reaction between an adsorbed methyl, or a methylene, group and an adsorbed CO.

References

[1] M. Ichikawa, J. Chem. Soc., Chem. Commun. (1978) 566.
[2] M. Ichikawa, K. Shikakura, in: Proceedings of the International Congress on Catalysis, Tokyo, Kindaska/Elsevier, Tokyo/Amsterdam, 1981, p. 925.
[3] V. Kutnetov, A. Romanenko, I. Mudrakovsky, V. Mathikhin, Y. Smachkov, Y. Yermakov, in: Proceedings of the International Congress on Catalysis, Berlin, 1984, Vol. V, VEB Chemie, Weinheim, 1982, p. 3.
[4] R. Bardet, J. Thivolle-Cazat, J. Trambouze, B. Imelik, et al. (Eds.), Metal Support and Metal Additive Effects in Catalysis, Elsevier, Amsterdam, 1982, p. 241.
[5] G. Van der Lee, B. Schuller, H. Post, T. Favre, V. Ponec, J. Catal. 98 (1986) 522.
[6] S. Chuang, Y. Tian, J. Goodwin, I. Wender, J. Catal. 96 (1985) 396.
[7] R.J. Katzer, A. Sleight, P. Gajardo, J. Michel, E. Gleason, S. McMillan, J. Chem. Soc. Faraday Disc. 72 (1982) 121.
[8] M. Ichikawa, Chemtech 11 (1982) 674.
[9] T. Tiruka, Y. Tanabe, J. Catal. 76 (1982) 1.
[10] R.P. Underwood, A.T. Bell, J. Catal. 111 (1988) 325.
[11] Du. Yu-Hua, Chen. De-An, Tsai. Khi-Rui, Appl. Catal. 35 (1987) 77.
[12] B.J. Kip, E.G.F. Hermans, J.H.M.C. Van Wolmput, N.M.A. Hermans, J. Van Grondelle, R. Prins, Appl. Catal. 35 (1987) 109.
[13] A. Benedetti, A. Carimati, S. Marengo, S. Martinengo, F. Pinna, R. Tessari, G. Strukul, T. Zerlia, L. Zanderighi, J. Catal. 122 (1990) 330.
[14] W.M.H. Sachtler, M. Ichikawa, J. Phys. Chem. 90 (1986) 4752.
[15] J.C. Lavalley, J. Saussey, J. Lamotte, R. Breault, J.P. Hindermann, A. Kiennemann, J. Phys. Chem. 94 (1990) 5941.
[16] M.N. Bredekhin, Yu.A. Lokhov, Kinet. Catal. 28 (1987) 678.
[17] M.N. Bredekhin, Yu.A. Lokhov, V.L. Kuznetzov, Kinet. Catal. 28 (1987) 671.
[18] S.A. Stevenson, A. Lisitsyn, H. Knozinger, J. Phys. Chem. 94 (1990) 1576.
[19] J.P. Hindermann, G.J. Hutchings, A. Kiennemann, Catal. Rev. Sci. Eng. 35 (1993) 1.
[20] D.E. Resasco, R.Y. Fenoguo, M.P. Suarez, J.O. Cechini, J. Phys. Chem. 90 (1986) 4330.
[21] C. Dall'Agnol, A. Gervasini, F. Morazzoni, F. Pinna, G. Strukul, L. Zanderighi, J. Catal. 96 (1985) 105.
[22] C. Mazzocchia, E. Tempesti, P. Gronchi, L. Giuffrè, L. Zanderighi, J. Catal. 111 (1988) 345.
[23] P. Casti, A. Amadè, Thesis, Politecnico di Milano, 1987.
[24] C. Mazzocchia, P. Gronchi, E. Tempesti, E. Guglielminotti, L. Zanderighi, J. Mol. Catal. 60 (3) (1990) 283.
[25] J.P. Hindermann, A. Kiennemann, S. Tazkritt, Stud. Surf. Sci. Catal. 48 (1989) 481.
[26] S. Borlini, Politecnico di Milano, Ph.D. Thesis, 1989.
[27] R.P. Underwood, A.T. Bell, J. Catal. 109 (1988) 61.
[28] A. Kiennemann, R. Breault, J.P. Hindermann, M. Laurin, J. Chem. Soc., Faraday Trans. 1 83 (1987) 2119.
[29] I. Mochida, N. Ikeyama, H. Ishibashi, H. Fujitsu, J. Catal. 110 (1988) 159.
[30] A.T. Bell, React. Kinet. Catal. Lett. 35 (1/2) 1987 107, and references therein.
[31] H. Orita, S. Naito, K. Tamaru, J. Catal. 111 (1988) 464.
[32] J.S. Rieck, A.T. Bell, J. Catal. 99 (1986) 278.
[33] F. Solymosi, H. Pasztor, J. Phys. Chem. 89 (1985) 4789.
[34] F. Solymosi, H. Pasztor, J. Phys. Chem. 90 (1986) 5312.
[35] F. Solymosi, I. Tombacz, M. Kocsis, J. Catal. 75 (1982) 78.